

2019

# A proposed mechanism of action of textile Al<sub>2</sub>O<sub>3</sub>-TiO<sub>2</sub> bimetal oxide nanocomposite as an antimicrobial agent

Shokoh Parham, *University Technology Malaysia*

Dedy H.B. Wicaksono, *Swiss German University*

Hadi Nur, *University Technology Malaysia*



## A proposed mechanism of action of textile/ $\text{Al}_2\text{O}_3$ - $\text{TiO}_2$ bimetal oxide nanocomposite as an antimicrobial agent

Shokoh Parham<sup>a</sup>, Dedy H. B. Wicaksono<sup>b</sup>  and Hadi Nur<sup>a,c</sup> 

<sup>a</sup>Centre for Sustainable Nanomaterials, Ibnu Sina Institute for Scientific and Industrial Research, Universiti Teknologi Malaysia, Johor, Malaysia; <sup>b</sup>Department of Biomedical Engineering, Faculty of Life Sciences and Technology, Swiss German University, EduTown BSD City, Tangerang, Indonesia; <sup>c</sup>Central Laboratory of Minerals and Advanced Materials, Faculty of Mathematics and Natural Sciences, State University of Malang, Malang, Indonesia

### ABSTRACT

The textile/ $\text{Al}_2\text{O}_3$ - $\text{TiO}_2$  bimetal oxide nanocomposite has been developed as an antimicrobial agent, but its antimicrobial mechanism has still not been clarified. The  $\text{Al}_2\text{O}_3$ - $\text{TiO}_2$  bimetal oxide nanoparticle has been reported as a radical scavenger. This study focuses on investigating the antimicrobial mechanism of the textile/ $\text{Al}_2\text{O}_3$ - $\text{TiO}_2$  bimetal oxide nanocomposite against *Escherichia coli* and their interaction with cell envelope biomolecules. L- $\alpha$ -Phosphatidyl ethanolamine (PE) is used as a model of bacteria to investigate the antimicrobial mechanism of this nanocomposite. The antimicrobial activity of the textile/ $\text{Al}_2\text{O}_3$ - $\text{TiO}_2$  bimetal oxide nanocomposite was investigated by using attenuated total reflectance/Fourier transform infrared (ATR-FTIR) and UV-Vis, while the toxicity of this nanocomposite was also examined through tissue culture test against a fibroblast skin cell. The ATR-FTIR used was able to confirm the destroyed cell envelope of the bacteria. The amounts of reactive oxygen species (ROS) were analyzed by UV-Vis spectroscopy and the toxicity of this nanocomposite was also examined by reacting tissue culture against the fibroblast skin cell. Overall, the antimicrobial mechanism of this textile nanocomposite was first by the attachment of this nanocomposite through the attachment of this nanoparticle to the surface of PE (as the model of bacteria) by hydrogen binding, and then nanoparticles can destroy the cell wall of bacteria through oxidation reaction by the produced ROS. Finally, these nanoparticles scavenged the ROS free radical. Therefore, the attached nanoparticles attached on textile can kill bacteria without any ROS free radical remaining in human body. These results suggest that the antimicrobial mechanism of this nanocomposite is mostly different due to the scavenger ability of this nanocomposite and its lower toxicity.

### ARTICLE HISTORY

Received 7 May 2017  
Accepted 14 September 2018

### KEYWORDS

Antimicrobial mechanism;  
textile/ $\text{Al}_2\text{O}_3$ - $\text{TiO}_2$  nanocomposite; radical scavenger

### Introduction

The reappearance of infectious diseases and the continuous development of antibiotic resistance among a variety of bacteria caused a serious problem to public health worldwide (Adams, Lyon, & Alvarez, 2006). Various new classes of  $\beta$ -lactamases have appeared, due to the broad use of  $\beta$ -lactam antibiotics in the clinical practice over the last several decades. The resistance to third-generation cephalosporin is now observed worldwide in all species of Enterobacteriaceae based on extended spectrum of  $\beta$  lactamases (ESBLs) especially in *Escherichia coli* (Bradford, 2001; Branger et al., 2005). Due to the ability of bacteria to cause resistance to almost all antibiotics, the antimicrobial therapy, morbidity, and mortality related with the bacterial infections remain high (Kolář, Urbánek, & Látal, 2001). Therefore new strategies are needed to develop and investigate next-generation antimicrobial agents or drugs to control the infection caused by bacteria. In this scenario, nano-sized materials have appeared as new antimicrobial agents due to their high surface area to volume ratio and unique physical and chemical

properties (Kim, Kim, & Cremer, 2001; Morones et al., 2005). Commonly, the harmful effects of such microorganisms that increase the undesirable effects of textile wound dressing can be prevented by using antimicrobial agents. Previous researchers have reported that metal oxide nanoparticle has toxicity for mammalian cell lines (Brunner et al., 2006), crustaceans (Heinlaan, Ivask, Blinova, Dubourguier, & Kahru, 2008), and bacteria (Adams et al., 2006). The nanosized metal oxides with a greater surface area than their bulk types show higher performance in their applications (Jiang, Mashayekhi, & Xing, 2009). Generally, the cell size of bacteria is in the micrometer range, while the pores of its outer cellular membranes are in the nanometer range. Therefore, the nanoparticles will have a unique ability of crossing the cell membrane when the size of nanoparticles is smaller than bacterial pores.

The antibacterial property of different nanoparticles depends on their size, stability, and concentration added to the growth medium, because this provides greater retention time for interaction between bacteria and nanoparticles. Due to the wide range of biomedical applications of

nanoparticles, for example in drug delivery, wound healing and imaging, the use of nanosized particles in clinical and experimental settings has increased. The nontoxicity and antimicrobial ability are two important key factors for biomedical applications like wound healing. In this setting, it is broadly accepted that cytotoxicity to animal or human cells depends on some parameters such as mechanism of antimicrobial action (Carré et al., 2014).

However, previous researcher reported that the cytotoxicity of some metal and metal oxide nanoparticles such as ZnO, TiO<sub>2</sub>, and Ag depends to the oxidative stress. This toxicity is dependent on the generation of reactive oxygen species (ROS) free radicals (Azam et al., 2012; Cioffi & Rai, 2012; Haghghi, Mohammadi, Mohammadi, Hosseinkhani, & Shipour, 2013; Iavicoli, Fontana, Leso, & Bergamaschi, 2013; Liu, Zhang, Fang, & Rong, 2014; Parham et al., 2016; Ravishankar & Jamuna Bai, 2011; Roy, Parveen, Koppalkar, & Prasad, 2010; Yun, Kim, Choi, & Lee, 2013). Previous researchers also reported that the toxicity of Al<sub>2</sub>O<sub>3</sub> and Al<sub>2</sub>O<sub>3</sub>-TiO<sub>2</sub> bimetal oxide are not high based on its role as radical scavenger and their ability to block ROS generation (Parham et al., 2016; Sadiq, Chowdhury, Chandrasekaran, & Mukherjee, 2009). The Al<sub>2</sub>O<sub>3</sub>-TiO<sub>2</sub> bimetal oxide nanoparticles in this nanocomposite can act as radical scavenger because Al<sub>2</sub>O<sub>3</sub> in this bimetal oxide nanoparticles has a  $\alpha$  structure (Parham et al., 2016). Therefore, the mechanism of action of this bimetal oxide nanoparticles is different with other structure of Al<sub>2</sub>O<sub>3</sub> nanoparticles such as  $\gamma$  structure (Ansari et al., 2014). Due to the scarcity of previously published reports on chemical and physical properties of metal and bimetal nanoparticles, there is few information on the antimicrobial or antibacterial properties of Al<sub>2</sub>O<sub>3</sub>-TiO<sub>2</sub> bimetal oxide nanoparticles and their textile nanocomposite, especially the mechanism of its antimicrobial action.

Besides, to control microbial infections, there is a pressing need to investigate novel strategies and to identify new antimicrobial agents from organic and inorganic materials. Therefore, in this study, the *E. coli* cell membrane biomolecules, specifically the L- $\alpha$ -Phosphatidylethanolamine (PE), are used as models to investigate the cellular interactions of Al<sub>2</sub>O<sub>3</sub>-TiO<sub>2</sub> bimetal oxide nanoparticles. PE is one of the major components of the outer membrane of Gram-negative (*E. coli*) and Gram-positive bacteria cells, and therefore it has been selected. Due to the absence of outer membrane, Gram-positive bacteria are more receptive to antimicrobial agents than Gram-negative bacteria such as *E. coli*. Therefore, in this study Gram-negative bacteria (*E. coli*) are used because it is more resistant to antimicrobial agents than Gram-positive bacteria. Thus, the overall goal of this study is to better understand Al<sub>2</sub>O<sub>3</sub>-TiO<sub>2</sub> bimetal oxide nanoparticles bacterial toxicity through nanoparticles-induced biomolecular changes and/or damage. The specific objectives of this study are to investigate the antimicrobial mechanism of textile/Al<sub>2</sub>O<sub>3</sub>-TiO<sub>2</sub> bimetal oxide nanocomposite by using ATR-FTIR to investigate the Al<sub>2</sub>O<sub>3</sub>-TiO<sub>2</sub> bimetal oxide nanoparticles-induced alterations/damage in surface molecules or functional groups.

## Experimental

### Materials

The material used in this study was textile/Al<sub>2</sub>O<sub>3</sub>-TiO<sub>2</sub> bimetal oxide nanocomposite (Parham et al., 2016). The L- $\alpha$ -Phosphatidyl-ethanolamine (PE) from Gram-negative bacteria *E. coli* (Sigma-Aldrich, St. Louis, MO) used for investigation the antimicrobial mechanism. The cytotoxicity test was carried out with human skin fibroblast (HSF 1184 catalogue no. 90011883, available from ECACC, Salisbury, UK), fetal bovine serum (FBS) (Sigma-Aldrich), phosphate buffered saline solution (PBS) (Sigma-Aldrich), minimum essential media (MEM) (catalogue no. 11095, Invitrogen, Carlsbad, CA), penicillin-streptomycin (PS) (Sigma-Aldrich), Hank's balanced salt solution (HBSS) (Sigma-Aldrich), trypsin/EDTA (Invitrogen), and the <sup>TM</sup>Red CMTPIX dye (Sigma-Aldrich) were also used.

### Methods

#### Investigation of antimicrobial mechanism

The textile/Al<sub>2</sub>O<sub>3</sub>-TiO<sub>2</sub> bimetal oxide nanocomposite and 5 mg of L- $\alpha$ -PE (the main phospholipid of bacteria's cell membrane) was added to the culture of *E. coli* at room temperature. Then, the solutions were centrifuged (40,000, 10 min). The toxicity of these solutions on human cell was analyzed with cell tissue or cell culture test. This experiment was repeated by using textile/TiO<sub>2</sub> nanocomposite instead of textile/Al<sub>2</sub>O<sub>3</sub>-TiO<sub>2</sub> bimetal oxide nanocomposite. This experiment was also repeated by using L- $\alpha$ -PE (the main phospholipid of bacteria's cell membrane), and the damaged structure of L- $\alpha$ -PE was analyzed by ATR-FTIR. The biomolecule samples were made by mixing 5 mg of L- $\alpha$ -PE with textile/Al<sub>2</sub>O<sub>3</sub>-TiO<sub>2</sub> nanocomposite in 25 mL distilled water or cell culture of *E. coli*, and the samples were shacked for 24 h. Then, a mixture of wet paste was obtained by centrifugation. After air-drying the wet paste on the top of the internal reflection element (IRE), a spectrum was obtained by collecting more than 200 scans with a spectral resolution of 2 cm<sup>-1</sup> and a scan speed of 0.5 cm/s. This experiment was repeated by using textile/TiO<sub>2</sub> nanocomposite (Kang & Xing, 2007).

**ROS analysis.** For analyzing the appearance of ROS, biomolecule samples were made by mixing 5 mg of L- $\alpha$ -PE with textile/Al<sub>2</sub>O<sub>3</sub>-TiO<sub>2</sub> nanocomposite in 25 mL cell culture of *E. coli*. Then, the reaction solutions were centrifuged (40,000 rpm, 10 min). Then the reaction solution was analyzed by liquid UV-Vis after 5 and 14 h, at room temperature. This experiment was repeated by using textile/TiO<sub>2</sub> nanocomposite. Then the reaction solution was analyzed by liquid UV-Vis after 14 h, at room temperature.

**Cell culture test.** Based on the Freshney protocol, HSF was cultured in MEM with 1% (v/v) PS, 10% (v/v) FBS and 2 mM glutamine (Freshney, 2005). The cell size was about 12 nm. The concentrations of attached cell cultures were retained at 2-9 × 10<sup>5</sup> cells per mL in a humidified incubator

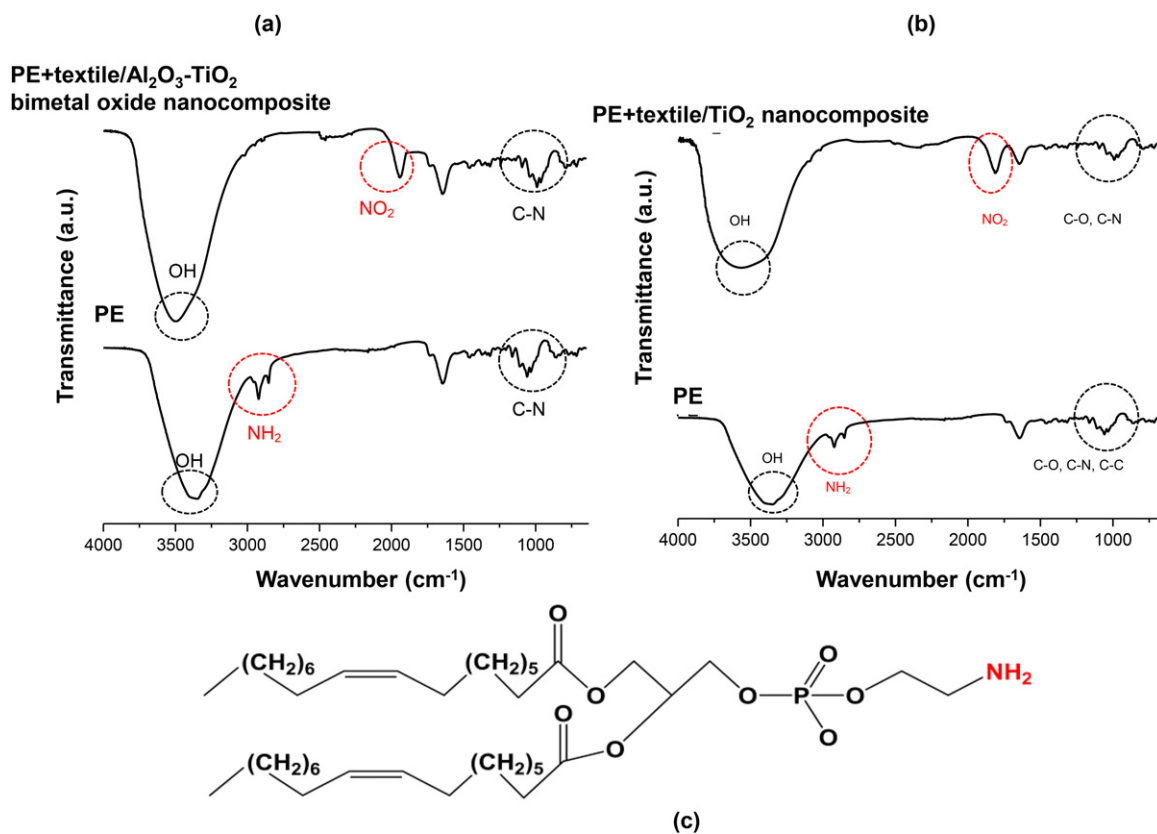


**Figure 1.** The ATR-FTIR spectra of PE and product reaction between (a) PE and textile/Al<sub>2</sub>O<sub>3</sub>-TiO<sub>2</sub> bimetal oxide nanocomposite and (b) PE and textile/TiO<sub>2</sub> nanocomposite. (c) The chemical structure of L- $\alpha$ -Phosphatidyl ethanolamine (PE).

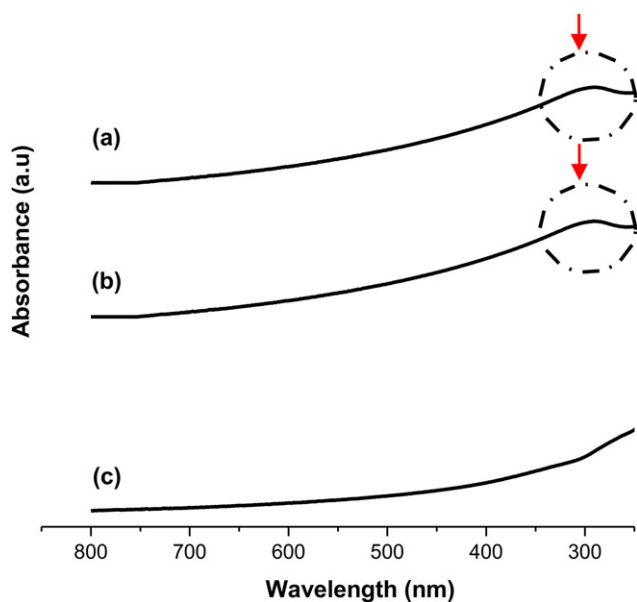


**Figure 2.** The UV-Vis spectra of solution reaction (a) after 14 h reaction between PE and textile/TiO<sub>2</sub> nanocomposite (b) after 5 h and (c) after 14 h reaction between PE and textile/Al<sub>2</sub>O<sub>3</sub>-TiO<sub>2</sub> bimetal oxide nanocomposite.

with 5% CO<sub>2</sub> at 37 °C. The cells reach to a confluence stage after 72 h and the cells passages were used; (P11–P15). When the cells are about 80% confluent, the cultures were washed by PBS. Then 0.25% trypsin/EDTA was used to detached the cells. To obtain cells pellets, the cells were centrifuged (at 2100 rpm for 5 min). The cells suspensions were used in 3 mL of MEM with a concentration of  $5 \times 10^5$  cells

per mL. Then <sup>TM</sup>Red CMTPX dye was used to stain the cell. The HSF cells in 12-well plates with or without samples were inserted into each well, 24 h before each experiment.

### Characterization

The damaged structure of L- $\alpha$ -PE was analyzed by ATR-FTIR (Nicolet IS10). The radical scavenging ability of the samples was measured by using a Shimadzu 1800 UV-visible spectrophotometer in the range of 250–800 nm.

## Results and discussion

### Antimicrobial mechanism

For achieve the antimicrobial mechanism of textile/Al<sub>2</sub>O<sub>3</sub>-TiO<sub>2</sub> bimetal oxide nanocomposite, the textile/Al<sub>2</sub>O<sub>3</sub>-TiO<sub>2</sub> bimetal oxide nanocomposite was added to PE. Figure 1(a) shows the ATR-FTIR spectrum of the reaction product between the textile/Al<sub>2</sub>O<sub>3</sub>-TiO<sub>2</sub> bimetal oxide nanocomposite and PE and Figure 1(b) shows the ATR-FTIR spectrum of the reaction product between the textile/TiO<sub>2</sub> bimetal oxide nanocomposite and PE. Figure 1(c) shows the chemical structure of L- $\alpha$ -PE. The ROS amount analysis is represented in Figure 2 while Figure 3 demonstrates the toxicity of these nanocomposites which is analyzed by tissue culture test against the fibroblast human skin cell.

The sample became a solution after 5 and 14 h whereby there was reaction between PE as the model with the textile/Al<sub>2</sub>O<sub>3</sub>-TiO<sub>2</sub> bimetal oxide nanocomposite (Figure 2(b,c)).

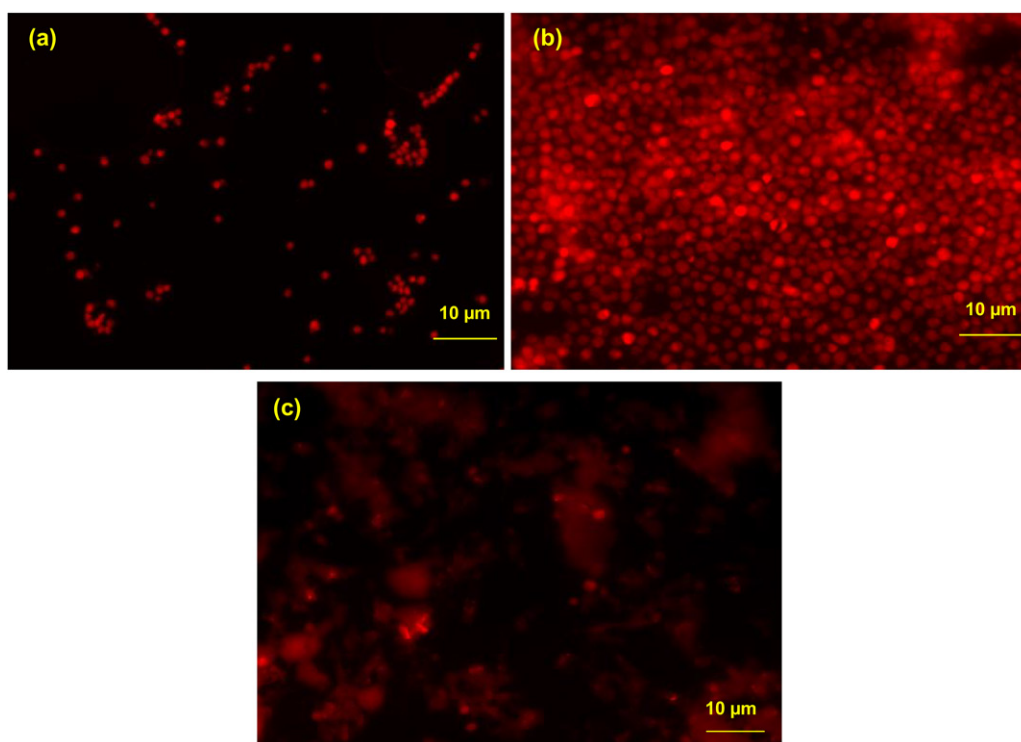


**Figure 3.** Histology of human skin fibroblasts grown on various cell medium solution of (a) after 5 h (b) after 14 h reaction between PE and textile/ $\text{Al}_2\text{O}_3$ - $\text{TiO}_2$  bimetal oxide nanocomposite (c) after 14 h reaction between PE and textile/ $\text{TiO}_2$  nanocomposite.

Therefore, based on this analyzed spectrum (Figure 2(b,c)) shows that after 5 h, a ROS was produced from the oxidation reaction between PE and the textile/ $\text{Al}_2\text{O}_3$ - $\text{TiO}_2$  bimetal oxide nanocomposite. Subsequently, after 5 h, the textile/ $\text{Al}_2\text{O}_3$ - $\text{TiO}_2$  bimetal oxide nanoparticles scavenged ROS free radicals (Figure 2(c)) from the reaction environment. Therefore, finally there were no more ROS free radicals in the solution. Figure 2(a) shows the amount of ROS that remained in the solution after 14 h' reaction between PE (as a model) and the textile/ $\text{TiO}_2$  nanocomposite. Therefore, based on this analyzed spectrum, a ROS was produced from the oxidation of PE with the textile/ $\text{TiO}_2$  nanocomposite. Thus, finally there were ROS free radicals in the reaction solution.

Compared with the results of other nanocomposites, the textile/ $\text{Al}_2\text{O}_3$ - $\text{TiO}_2$  bimetal oxide nanocomposite shows the best result. The fibroblast human skin cell can be grown onto standard tissue culture with a reaction solution between PE and the textile/ $\text{Al}_2\text{O}_3$ - $\text{TiO}_2$  bimetal oxide nanocomposite after 5 and 14 h, showing similar morphologies and densities (refer Figure 3). The cell shape was globular and the cell density high. The cell density is higher than in other textile compositions because the radical scavenging ability of this textile nanocomposite is higher than other samples. Therefore, based on current literature, there was no toxicity in the absence of ROS free radicals (Beneš, Ďuračková, & Ferencik, 1999; Wu & Cederbaum, 2003). Based on Figure 3, this confirmed the result of the UV-Vis spectrum. With that, all results represented that this textile nanocomposite did not show any toxicity for the fibroblast human skin cell. Figure 3(c) highlights the histology of the fibroblast human skin cell grown in standard tissue culture

with a reaction solution between PE and the textile/ $\text{TiO}_2$  metal oxide nanocomposite (after 14 h' interaction). The cell shape was not globular and the cell wall was completely destroyed in the solution after 14 h of antimicrobial interaction. This phenomenon is related to the antimicrobial mechanism of this nanocomposite. However, the antimicrobial mechanism of the nanoparticles created oxidative stress *via* the generation of ROS, with lipid peroxidation that caused the enhancement of membrane fluidity and disruption of the cell wall (Besinis, De Peralta, & Handy, 2014).

PE is the principal bacterial phospholipid. In Figure 1, the strong absorption at  $1740\text{ cm}^{-1}$  was from the C=O of ester carbonyl (Lewis & McElhaney, 2007). For the observed PE, the C=O stretching band was noted to be a summation of at least two major components that are usually near  $1738$ – $1742$  and  $1724$ – $1729\text{ cm}^{-1}$ , reflecting the differences in the degrees of hydration or hydrogen bonding to the ester carbonyl groups (Greenhall, Yarwood, Brown, & Swart, 1998; Lewis & McElhaney, 1998). The textile/ $\text{Al}_2\text{O}_3$ - $\text{TiO}_2$  bimetal oxide nanocomposite slightly shifted C=O from  $1740$  to  $1736\text{ cm}^{-1}$  (refer Figure 1). The shift may be due to the hydrogen bonding of the ester carbonyl group on the nanocomposite surface (Greenhall et al., 1998). The C=O remained in the ester frequency region (Bellamy, 1975; Socrates, 2001), therefore, the ester bond was not broken by the nanoparticles.

The bands at  $1636$  and  $1533\text{ cm}^{-1}$  (refer Figure 1) were due to deformation of  $\text{RNH}_3^+$  or  $\text{RNH}_2$  (Bellamy, 1975; Socrates, 2001). The two bands around  $3000\text{ cm}^{-1}$  belong to  $\text{NH}_2$  (the primary amine). These two bands disappeared when PE absorb all the nanocomposites, due perhaps to the interaction of the PE amine moiety with the metal oxide

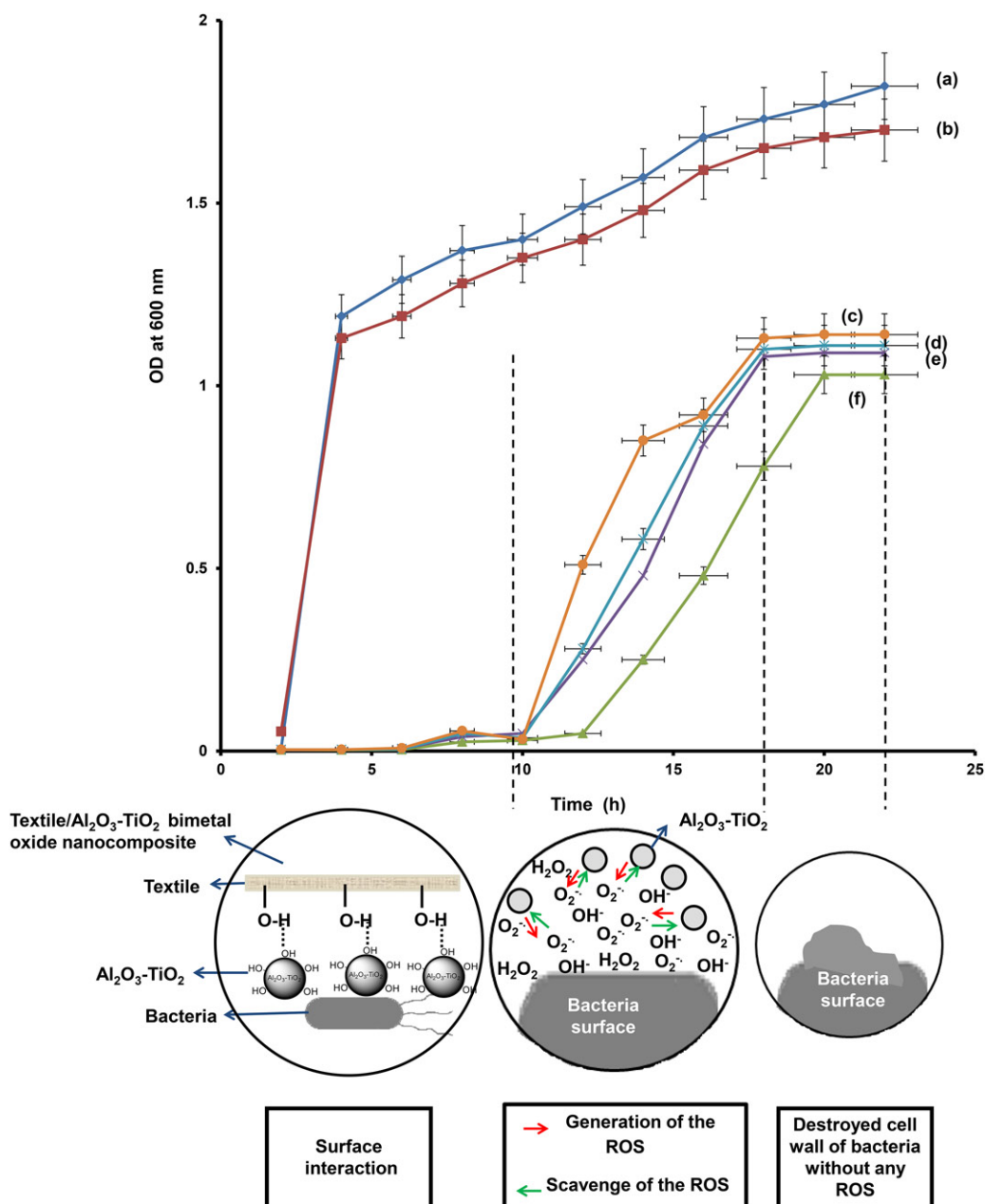


**Figure 4.** The antimicrobial mechanism of textile/ $\text{Al}_2\text{O}_3\text{-TiO}_2$  bimetal oxide nanocomposite based on Growth curve of *E. coli* on textile/ $\text{Al}_2\text{O}_3\text{-TiO}_2$  bimetal oxide nanocomposite in different concentrations (75, 100, 125, and 150 mmol/L) in liquid medium by optical density (OD) at 600 nm: (a) culture *E. coli*, (b) textile, (c) 75 mmol/L, (d) 100 mmol/L, (e) 125 mmol/L, and (f) 150 mmol/L.

surface. The new peak formed at near  $2000\text{ cm}^{-1}$  and belonged to the  $\text{NO}_2$  group. Therefore, formation of this peak shows oxidation of PE by this nanoparticle.

Absorption bands between  $1200$  and  $1250\text{ cm}^{-1}$  (refer Figure 1) resulted from the  $\text{PO}_2^-$  in phosphodiester (Omoike & Chorover, 2004). The frequency is at about  $1220\text{ cm}^{-1}$  when the phosphodiester group is fully hydrogen-bonded, and at  $1240\text{ cm}^{-1}$  and above when the phosphodiester group is non-hydrogen-bonded (Wong, Papavassiliou, & Rigas, 1991). The peaks of  $\text{PO}_2^-$  at  $1094\text{--}1084\text{ cm}^{-1}$  (Kinder, Ziegler, & Wessels, 1997; Lewis & McElhaney, 2007) overlapped with the bands arising from C—N, C—O, C—O—C, and C—O—P stretching modes (Parikh & Chorover, 2006; Socrates, 2001), but had a shoulder peak at  $1091\text{ cm}^{-1}$ . Due to the diminishing peak at

$1078\text{ cm}^{-1}$  after the PE absorbed the nanocomposite, a sharp ( $\text{PO}_2^-$ ) peak emerged at  $1091\text{ cm}^{-1}$  (refer Figure 1).

The absorbance at  $1063\text{ cm}^{-1}$  was assigned to the C—O—C (Greenhall et al., 1998; Kiwi & Nadochenko, 2005), and emerged due to the diminishment of absorbance at  $1078\text{ cm}^{-1}$ . The peak at  $1078\text{ cm}^{-1}$  was assigned to P=O (Badireddy et al., 2008) and its reduction may be from the phosphodiester breaking or phosphate moiety absorption of the nanocomposites. The broad peak around  $3300$  resulted from the OH group. When PE was attached to the nanocomposite by the hydrogen band, this band shifted to a lower frequency.

Infrared (IR) spectral changes revealed that the structure of PE could be oxidized by these nanoparticles such as  $\text{Al}_2\text{O}_3\text{-TiO}_2$  bimetal oxide. Nanoparticles produced a ROS

**Table 1.** The textile/ $\text{Al}_2\text{O}_3$ - $\text{TiO}_2$  bimetal oxide nanocomposite and textile/ $\text{TiO}_2$  nanocomposite used as antimicrobial agents together with their antimicrobial mechanisms.

Textile nanocomposite	Proposed mechanism of antimicrobial action	The main factors that influence antimicrobial activity
Textile/ $\text{TiO}_2$ nanocomposite	Oxidative stress <i>via</i> the generation of ROS; lipid peroxidation that cause to improve membrane fluidity and disruption of the cell wall	Shape, size, and crystal structure
Textile/ $\text{Al}_2\text{O}_3$ - $\text{TiO}_2$ nanocomposite	The ROS generation, lipid peroxidation that cause to improve membrane fluidity and disruption of the cell wall and then scavenge the ROS therefore low toxicity	Crystal structure

that creates free radicals by oxidation reaction. These nanoparticles could change the chemical structure of PE that could bind to these nanoparticles through hydrogen binding. These nanoparticles when induced could cause structural changes in phospholipids. It may lead to the loss of amphiphilic properties. It may also bring about the destruction of the membrane and leaking of the cell. When the nanoparticles can penetrate the membrane, and accumulate inside the bacterial cell, it causes pit formation, perforation, disorganization, and finally, this disturbed its proper function. Biomolecular changes on the cell surface revealed by the ATR-FTIR spectra provide a better understanding of the cytotoxicity of these nanoparticles. Based on Figure 4, the antimicrobial mechanism of the textile/ $\text{Al}_2\text{O}_3$ - $\text{TiO}_2$  bimetal oxide nanocomposite goes through several different steps. The attachment of this nanocomposite through the attachment of  $\text{Al}_2\text{O}_3$ - $\text{TiO}_2$  bimetal oxide nanoparticles to the surface of PE (as the model of bacteria) is by hydrogen binding. Then, these nanoparticles oxidize the cell wall of the bacteria, by producing a ROS. These nanoparticles induced structural changes in the phospholipids which may lead to the loss of amphiphilic properties, destruction of the membrane and leaking from the cell. Therefore, the penetration and accumulation of nanoparticles inside the bacterial cell cause pit formation, perforation, and disorganization, and thus drastically disturb its proper function. For the textile/ $\text{Al}_2\text{O}_3$ - $\text{TiO}_2$  bimetal oxide nanocomposite, ROS free radicals are scavenged by the special structure of  $\text{Al}_2\text{O}_3$ - $\text{TiO}_2$  bimetal oxide. Since  $\text{Al}_2\text{O}_3$ - $\text{TiO}_2$  bimetal oxide are radical scavengers, this can directly inhibit the production of ROS, which can rapidly induce the ROS defense system to be activated before the program of cell degradation is complete. Figure 4 shows the antimicrobial mechanism of the textile/ $\text{Al}_2\text{O}_3$ - $\text{TiO}_2$  bimetal oxide nanocomposite for all steps based on growth curve of *E. coli* on textile/ $\text{Al}_2\text{O}_3$ - $\text{TiO}_2$  bimetal oxide nanocomposite in different concentrations (75, 100, 125, and 150 mmol/L) in liquid medium. Figure 4 demonstrates the growth cells of bacteria. There is the relation between growth cells of bacteria and number of cells of bacteria, when the growth cells of bacteria are high, the number of bacteria's cells is also high and when the growth cells of bacteria are low, the number of bacteria's cells is also low.

Table 1 shows the textile/ $\text{Al}_2\text{O}_3$ - $\text{TiO}_2$  bimetal oxide nanocomposite and textile/ $\text{TiO}_2$  nanocomposite used as antimicrobial agents together with their antimicrobial mechanisms. The antimicrobial property of  $\text{TiO}_2$  nanoparticles is related to its size, shape, and crystal structure (Haghighi et al., 2013). A particularly important proposed mechanism

for  $\text{TiO}_2$  nanoparticles is the oxidative stress *via* the generation of ROS. ROS will then cause damage to the site-specific DNA and structure of the cell wall ROS is very toxic and it can be caused to cancer (Fu, Xia, Hwang, Ray, & Yu, 2014). Therefore, based on Table 1, the antimicrobial mechanism of this nanocomposite is mostly different due to scavenger ability of this nanocomposite and lower toxicity.

Therefore, there are no ROS free radicals in the human body for the textile/ $\text{Al}_2\text{O}_3$ - $\text{TiO}_2$  bimetal oxide nanocomposite. In order to confirm this result, the reaction solution was tested by the fibroblast human skin cell. The result is represented in Figure 3, where it can be noted that the antimicrobial mechanism of the textile/ $\text{Al}_2\text{O}_3$ - $\text{TiO}_2$  bimetal oxide nanocomposite was first on the surface interaction between the bacteria and nanoparticles, and then the nanoparticles destroyed the cell wall of the bacteria through the oxidation reaction produced by ROS. Finally, these nanoparticles scavenged the ROS free radicals. Therefore, these nanoparticles attached on the textile can destroy the bacteria without any ROS free radicals remaining in the human body. Conclusively, it can be used as a potential for wound dressing to reduce wounds' infection.

## Conclusion

Overall, the textile/ $\text{Al}_2\text{O}_3$ - $\text{TiO}_2$  bimetal oxide's antimicrobial mechanism has been successfully investigated by using L- $\alpha$ -PE of bacteria's cell membrane as a model compound. ATR-FTIR studies have suggested the interaction of PE with this nanocomposite. The intracellular  $\text{Al}_2\text{O}_3$ - $\text{TiO}_2$  bimetal oxide nanoparticles might have interacted with cellular biomolecules and caused adverse effects eventually triggering the bacteria cell death. IR spectral changes revealed that the PE could bind to these nanoparticles through hydrogen binding. This nanoparticle-induced structural changes in phospholipids may lead to the loss of amphiphilic properties, destruction of the membrane and cell leaking. Therefore, the antimicrobial mechanism of this textile nanocomposite was first by the attachment of this nanocomposite through the attachment of  $\text{Al}_2\text{O}_3$ - $\text{TiO}_2$  bimetal oxide nanoparticles to the surface of PE (as the model of bacteria) by hydrogen binding. Then the nanoparticles destroy the cell wall of bacteria through oxidation reaction by producing ROS. Finally, these nanoparticles scavenged the ROS free radical. Therefore, these attached nanoparticles on textile can kill bacteria without any remaining ROS free radical in human body. The results of using PE as a bacteria cell wall model represented the antimicrobial mechanism of this nanocomposite. These results suggest that the antimicrobial

mechanism of this nanocomposite is mostly different due to scavenger ability of this nanocomposite and its lower toxicity. The outstanding features of the results indicate that this textile nanocomposite can be used as a potential wound dressing to improve infectious wounds and to improve wound-healing process.

## Acknowledgment

The authors would like to express gratitude of Universiti Teknologi Malaysia (UTM) for support.

## Disclosure statement

No potential conflict of interest was reported by the authors.

## Funding

H. Nur acknowledges funding from the Ministry of Education (MOE) under the Long Term Research Grant Scheme (R.K130000.734004L825) and FRGS grant no. FRGS/2/2014/SG06/UTM/01/1. D. H. B. Wicaksono would like to acknowledge Central Research Fund (CRF) and Faculty Research Fund (FRF) from Swiss German University (SGU).

## ORCID

Dedy H. B. Wicaksono  <http://orcid.org/0000-0003-1218-6853>  
Hadi Nur  <http://orcid.org/0000-0002-4387-431X>

## References

- Adams, L. K., Lyon, D. Y., & Alvarez, P. J. (2006). Comparative ecotoxicity of nanoscale TiO<sub>2</sub>, SiO<sub>2</sub>, and ZnO water suspensions. *Water Research*, 40(19), 3527–3532. doi:10.1016/j.watres.2006.08.004
- Ansari, M. A., Khan, H. M., Khan, A. A., Cameotra, S. S., Saquib, Q., & Musarrat, J. (2014). Interaction of Al<sub>2</sub>O<sub>3</sub> nanoparticles with *Escherichia coli* and their cell envelope biomolecules. *Journal of Applied Microbiology*, 116(4), 772–783. doi:10.1111/jam.12423
- Azam, A., Ahmed, A. S., Oves, M., Khan, M. S., Habib, S. S., & Memic, A. (2012). Antimicrobial activity of metal oxide nanoparticles against gram-positive and gram-negative bacteria: A comparative study. *International Journal of Nanomedicine*, 7, 6003–6009. doi:10.2147/IJN.S35347
- Badireddy, A. R., Korpil, B. R., Chellam, S., Gassman, P. L., Engelhard, M. H., Lea, A. S., & Rosso, K. M. (2008). Characterization of extracellular polymeric substance from *Escherichia coli* and *Serratia marcescens*: Suppression using subinhibitory concentrations of bismuth thiols. *Biomacromolecules*, 9(11), 3079–3089. doi:10.1021/bm800600p
- Bellamy, L. J. (1975). *The infra-red spectra of complex molecules*. London: Chapman and Hall London.
- Besinis, A., De Peralta, T., & Handy, R. D. (2014). The antibacterial effects of silver, titanium dioxide and silica dioxide nanoparticles compared to the dental disinfectant chlorhexidine on *Streptococcus mutans* using a suite of bioassays. *Nanotoxicology*, 8(1), 1–16. doi:10.3109/17435390.2012.742935
- Bradford, P. A. (2001). Extended-spectrum β-lactamases in the 21st century: Characterization, epidemiology, and detection of this important resistance threat. *Clinical Microbiology Reviews*, 14(4), 933–951. doi:10.1128/CMR.14.4.933-951.2001
- Branger, C., Zamfir, O., Geoffroy, S., Laurans, G., Arlet, G., Thien, H. V., ... Denamur, E. (2005). Genetic background of *Escherichia coli* and extended-spectrum beta-lactamase type. *Emerging Infectious Diseases*, 11(1), 54–61. doi:10.3201/eid1101.040257
- Brunner, T. J., Wick, P., Manser, P., Spohn, P., Grass, R. N., Limbach, L. K., ... Stark, W. J. (2006). In vitro cytotoxicity of oxide nanoparticles: Comparison to asbestos, silica, and the effect of particle solubility. *Environmental Science & Technology*, 40(14), 4374–4381. doi:10.1021/es052069i
- Carré, G., Hamon, E., Ennahar, S., Estner, M., Lett, M. C., Horvatovich, P., ... Andre, P. (2014). photocatalysis damages lipids and proteins in *Escherichia coli*. *Applied and Environmental Microbiology*, 80(8), 2573–2581. doi:10.1128/AEM.03995-13
- Cioffi, N., & Rai, M. (2012). *Nano-antimicrobials: Progress and prospects*. Berlin: Springer.
- Freshney, R. I. (2005). *Culture of specific cell types*. Hoboken, NJ: Wiley Online Library.
- Fu, P. P., Xia, Q., Hwang, H. M., Ray, P. C., & Yu, H. (2014). Mechanisms of nanotoxicity: Generation of reactive oxygen species. *Journal of Food and Drug Analysis*, 22(1), 64–75. doi:10.1016/j.jfda.2014.01.005
- Greenhall, M., Yarwood, J., Brown, R., & Swart, R. (1998). Spectroscopic studies of model biological membranes in vesicles and Langmuir-Blodgett films. *Langmuir*, 14(10), 2619–2626. doi:10.1021/la970458n
- Haghighi, F. R., Mohammadi, S., Mohammadi, P., Hosseinkhani, S., & Shipour, R. (2013). Antifungal activity of TiO<sub>2</sub> nanoparticles and EDTA on *Candida albicans* biofilms. *Infection, Epidemiology and Medicine*, 1(1), 33–38.
- Heinlaan, M., Ivask, A., Blinova, I., Dubourguier, H. C., & Kahru, A. (2008). Toxicity of nanosized and bulk ZnO, CuO and TiO<sub>2</sub> to bacteria *Vibrio fischeri* and crustaceans *Daphnia magna* and *Thamnocephalus platyurus*. *Chemosphere*, 71(7), 1308–1316. doi:10.1016/j.chemosphere.2007.11.047
- Iavicoli, I., Fontana, L., Leso, V., & Bergamaschi, A. (2013). The effects of nanomaterials as endocrine disruptors. *International Journal of Molecular Sciences*, 14(8), 16732–16801. doi:10.3390/ijms140816732
- Jiang, W., Mashayekhi, H., & Xing, B. (2009). Bacterial toxicity comparison between nano-and micro-scaled oxide particles. *Environmental Pollution*, 157(5), 1619–1625. doi:10.1016/j.envpol.2008.12.025
- Kang, S., & Xing, B. (2007). Adsorption of dicarboxylic acids by clay minerals as examined by in situ ATR-FTIR and ex situ DRIFT. *Langmuir*, 23(13), 7024–7031. doi:10.1021/la700543f
- Kim, J., Kim, G., & Cremer, P. S. (2001). Investigations of water structure at the solid/liquid interface in the presence of supported lipid bilayers by vibrational sum frequency spectroscopy. *Langmuir*, 17(23), 7255–7260. doi:10.1021/la0017274
- Kinder, R., Ziegler, C., & Wessels, J. M. (1997). Gamma-irradiation and UV-C light-induced lipid peroxidation: A Fourier transform-infrared absorption spectroscopic study. *International Journal of Radiation Biology*, 71(5), 561–571. doi:10.1080/095530097143897
- Kiwi, J., & Nadochenko, V. (2005). Evidence for the mechanism of photocatalytic degradation of the bacterial wall membrane at the TiO<sub>2</sub> interface by ATR-FTIR and laser kinetic spectroscopy. *Langmuir*, 21(10), 4631–4641. doi:10.1021/la046983l
- Kolář, M., Urbánek, K., & Látal, T. (2001). Antibiotic selective pressure and development of bacterial resistance. *International Journal of Antimicrobial Agents*, 17(5), 357–363. doi:10.1016/S0924-8579(01)00317-X
- Lewis, R. N., & McElhaney, R. N. (1998). The structure and organization of phospholipid bilayers as revealed by infrared spectroscopy. *Chemistry and Physics of Lipids*, 96(1–2), 9–21. doi:10.1016/S0009-3084(98)00077-2
- Lewis, R. N., & McElhaney, R. N. (2007). Fourier transform infrared spectroscopy in the study of lipid phase transitions in model and biological membranes. *Methods in Membrane Lipids*, 207, 226.
- Liu, Q., Zhang, M., Fang, Z. X., & Rong, X. H. (2014). Effects of ZnO nanoparticles and microwave heating on the sterilization and product quality of vacuum-packaged Caixin. *Journal of the Science of Food and Agriculture*, 94(12), 2547–2554. doi:10.1002/jsfa.6594

- Morones, J. R., Elechiguerra, J. L., Camacho, A., Holt, K., Kouri, J. B., Ramírez, J. T., & Yacaman, M. J. (2005). The bactericidal effect of silver nanoparticles. *Nanotechnology*, 16(10), 2346. doi:10.1088/0957-4484/16/10/059
- Omoike, A., & Chorover, J. (2004). Spectroscopic study of extracellular polymeric substances from *Bacillus subtilis*: Aqueous chemistry and adsorption effects. *Biomacromolecules*, 5(4), 1219–1230. doi:10.1021/bm034461z
- Parham, S., Chandren, S., Wicaksono, D. H., Bagherbaigi, S., Lee, S. L., Yuan, L. S., & Nur, H. (2016). Nanocomposite as an antimicrobial and radical scavenger wound dressing. *RSC Advances*, 6(10), 8188–8197. doi:10.1039/C5RA20361A
- Parikh, S. J., & Chorover, J. (2006). ATR-FTIR spectroscopy reveals bond formation during bacterial adhesion to iron oxide. *Langmuir*, 22(20), 8492–8500. doi:10.1021/la061359p
- Ravishankar Rai, V., & Jamuna Bai, A. (2011). *Nanoparticles and their potential application as antimicrobials: Science against microbial pathogens: Communicating current research and technological advances*. Spain: Formatex Research Center.
- Roy, A. S., Parveen, A., Koppalkar, A. R., & Prasad, M. A. (2010). Effect of nano-titanium dioxide with different antibiotics against methicillin-resistant *Staphylococcus aureus*. *Journal of Biomaterials and Nanobiotechnology*, 01(01), 37–41. doi:10.4236/jbnb.2010.11005
- Sadiq, I. M., Chowdhury, B., Chandrasekaran, N., & Mukherjee, A. (2009). Antimicrobial sensitivity of *Escherichia coli* to alumina nanoparticles. *Nanomedicine: Nanotechnology, Biology and Medicine*, 5(3), 282–286. doi:10.1016/j.nano.2009.01.002
- Socrates, G. (2001). *Infrared and Raman characteristic group frequencies*. Hoboken, NJ: John Wiley and Sons.
- Wong, P., Papavassiliou, E., & Rigas, B. (1991). Phosphodiester stretching bands in the infrared spectra of human tissues and cultured cells. *Applied Spectroscopy*, 45(9), 1563–1567. doi:10.1366/0003702914335580
- Wu, D., & Cederbaum, A. I. (2003). Alcohol, oxidative stress, and free radical damage. *Alcohol Research Health*, 27(4), 277–284.
- Yun, H., Kim, J. D., Choi, H. C., & Lee, C. W. (2013). Antibacterial activity of CNT-Ag and GO-Ag nanocomposites against gram-negative and gram-positive bacteria. *Bulletin of the Korean Chemical Society*, 34(11), 3261. doi:10.5012/bkcs.2013.34.11.3261